IOPscience iopscience.iop.org

Home Search Collections Journals About Contact us My IOPscience

Comparison of strain fields in truncated and un-truncated quantum dots in stacked InAs/GaAs nanostructures with varying stacking periods

This article has been downloaded from IOPscience. Please scroll down to see the full text article.

2003 J. Phys.: Condens. Matter 15 3689

(http://iopscience.iop.org/0953-8984/15/22/304)

View the table of contents for this issue, or go to the journal homepage for more

Download details:
IP Address: 94.79.44.176
The article was downloaded on 19/05/2010 at 09:59

Please note that terms and conditions apply.

INSTITUTE OF PHYSICS PUBLISHING JOURNAL OF PHYSICS: CONDENSED MATTER

J. Phys.: Condens. Matter **15** (2003) 3689–3699 PII: S0953-8984(03)59287-6

Comparison of strain fields in truncated and un-truncated quantum dots in stacked InAs/GaAs nanostructures with varying stacking periods

Hyunho Shin, Woong Lee and Yo-Han Yoo[1]

1st R&D Centre, Agency for Defence Development, Yuseong, PO Box 35-1, Daejeon, 305-600, Republic of Korea

E-mail: yyhh1986@kornet.net

Received 3 February 2003
Published 23 May 2003
Online at stacks.iop.org/JPhysCM/15/3689

Abstract
Strain fields in truncated and un-truncated InAs quantum dots with the same height and base length have been compared numerically when the dots are vertically stacked in a GaAs matrix at various stacking periods. The compressive hydrostatic strain in truncated dots decreases slightly as compared with the un-truncated dots without regard to the stacking period studied. However, the reduction in tensile biaxial strain, compressive radial strain and tensile axial strain was salient in the truncated dot and the reduction increased with decreasing stacking period. From such changes in strain, changes in the band gap and related properties are anticipated.

1. Introduction

The three-dimensionally confined quantum dot shows unique properties as compared with bulk, one-dimensionally confined (quantum well) or two-dimensionally confined (quantum wire) structures. For instance, the dot yields atom-like electronic states, e.g. discrete energy levels [1] within the band gap of the matrix material, and thus it has received considerable attention for opto-electronic applications [2, 3]. The most-studied quantum dot system today is based on InAs (or $In_xGa_{1-x}As$) quantum dots in a GaAs matrix fabricated by various processing techniques [4–8].

The lattice mismatch strain between an InAs dot and GaAs matrix is 6.7% and this inherent strain is accommodated in the quantum dot structure entirely elastically without plastic relaxation via formation of crystal defects such as dislocations. The reported shapes of InAs quantum dots embedded in GaAs are more or less pyramidal: lens-like shape, pyramid or truncated pyramid. The difference in the truncated or un-truncated state in the dot-embedded structure certainly results in a change in the strain field [9, 10].

[1] Author to whom any correspondence should be addressed.

© 2003 IOP Publishing Ltd Printed in the UK

The strain field in or around the quantum dot results in a change in electronic structure and therefore in the opto-electronic properties of the dot by modifying the energies and wavefunctions for confined carriers [11]. The hydrostatic component of strain ε_{hyd}, for example, usually shifts the conduction and valence band edges while biaxial strain ε_{bi} modifies the valence bands by splitting the degeneracy of the light- and heavy-hole bands [12]. Hence studies in the strain field in or around a quantum dot with either a truncated or un-truncated shape have received much interest from many researchers [8–10, 13–20].

For practical device applications, quantum dots are vertically stacked to form multi-layers for a high spatial density of dots and an optimal device performance [21]. In the case of laser applications, for instance, stacking yields a higher modal gain. Such a narrow vertical stacking, i.e. a vertical periodicity of less than several nanometres, seems to result in a change in physical properties perhaps associated with the strain field interaction between the dots [22], since the strain field from each quantum dot extends up to about 40 nm [23]. Since strain field interaction in a narrow-stacked structure would depend on the shape of the dot, i.e. whether it is truncated or not, a comparative understanding of the strain field interaction for different dot shapes is of importance. However, most previous research on the strain field have focused on the unstacked single-layered dot state [8–10, 13–19] and not much work has been performed for the multi-stacked structure [20]. In a recent analytical work [20], the strains for truncated and un-truncated dots are reported for the stacked structure, whilst neither a quantitative comparison of the influence of dot truncation on strain change is addressed nor the information of strain change, especially for different stacking periods, is available since the strains were calculated at a specific stacking period. Thus, in the present work, the strain field in or around the dot due to strain field interaction in a series of multi-stacked structure has been quantitatively studied for the two different shapes of the quantum dot, i.e. truncated and un-truncated shapes, and the change with dot truncation is reported as a function of the stacking period.

Many methods of modelling quantum dot hetero-structures have been developed to analyse the strain field. The methods are categorized largely into two groups. The first group is the atomistic approach [24–28] utilizing atomic potentials. Perhaps this approach provides the most accurate results, while it demands extensive computational resources and thus has been utilized for relatively simple structures such as unstacked single layered dot structure. The second is based on the continuum elasticity (CE) assumption. This approach has been experimentally verified to be valid for layers as thin as the monolayer level [29, 30]. In theoretical works comparing different numerical methodologies [26–28], the CE and atomistic approaches showed good agreement for a layer whose thickness was of the order of five atoms. A subtle difference was observed only in regions where strain was changing rapidly, namely the edge of the structure, implying that the CE approach is very cost efficient [26–28].

The CE approach, in turn, can be divided into two categories. The first one is the analytical method based on Eshelby's inclusion theory [31] under the assumptions of elastic isotropy and uniformity of elastic properties. Although this method has been extended to handle more complicated geometry of inclusions such as pyramids, it treats inclusions in an infinite medium [9, 19, 20], and also the accommodation of anisotropic properties are difficult [32]. Thus this may not be appropriate for our purpose, which focuses on the vertically stacked multi-dots especially with varying stacking periodicity in the vertical direction and lateral periodicity. The second CE approach for nanostructures is the numerical method. This generally utilizes the finite difference [8] or finite element methods [10, 13–18]. Much research on the strain field of the single dot structure has been performed by the finite element method and the validity of finite element analysis has been reported based on experiments [33]. It is appropriate especially for complex geometries like the stacked multi-dots while it requires less computational resources

than the atomistic approach. Thus the finite element method based on the CE has been utilized in the present study.

2. Numerical analysis

The reported shapes of InAs quantum dots embedded in GaAs have been hemispherical [34], multifaceted domes [34] or a lens-like shape [6, 7, 22], whilst several other groups reported dots with pyramidal shapes [8] or truncated pyramids [35]. It has been raised, based on detailed contrast evidence, that there is a possibility that some different geometric features may result from an illusion induced by strain fields in TEM observations [36]. The quantum dots are often modelled in axial symmetry, i.e. conical dots [14–18] in numerical calculations of the strain field because the time-consuming three-dimensional calculations (with other dot shapes) give no significantly different results [10, 15]. This work utilizes the axisymmetric geometry.

Figure 1 shows the half-space of the multi-layer-stacked geometry with un-truncated and truncated dots modelled for the finite element analysis. The base and height of the InAs dot were 20 and 4.3 nm, respectively, and the GaAs cap layer and buffer were 55 and 50 nm thick, respectively. The modelled vertical periods of the dot P were 5.5, 6.0, 7.0, 8.0 and 10 nm. The range of the investigated period herein has been selected on the basis that a period beyond about half of the base length of the dot (10 nm in this paper) did not guarantee vertical stacking during processing while too close a spacing resulted in a severe distortion of the stacked structure [37]. The lower limit period, 5.5 nm, selected here is based on the experimental observation that there seems to be a slight distortion of the stacked structure in this case [6, 7]. The reference state of the dot structures with varying stacking period was selected in this work as the structure with a period of infinity. This was simulated by replacing the multi-layer with an unstacked single layer for each type of dot. The free boundary at the bottom and top of the model did not result in any appreciable change in strain field in or around the single-layered dot when the thickness of the cap layer and buffer layer was more than about 50 nm, indicating that the single-layered model effectively simulates a period of infinity.

The base length, height and period of 5.5 nm were based on experimental observations elsewhere [6, 7]. Since the shape of the vertex of the experimentally observed dot with $P = 5.5$ nm was not unambiguous, although the base and height of the dot are relatively clear, as is often the case for other nano-scaled dot structures, the apex shape of the dot is assumed to be either un-truncated or truncated in this work for modelling and comparison purposes. The strain fields in such two different geometries with the same height were also compared in the unstacked structure in the literature [9, 10] and thus would provide a comparison standard for the present work. Although the dot geometries in the current work are modelled based on the two different possibilities of experimental observation, recent progress in processing allows truncation of the dot in the stacked structure [38], indicating that comparison of the strain field for the two different dot geometries is of importance.

Although about ten dot layers were fabricated in experiments, only seven layers were modelled in the present work for simplicity because, in a separate preliminary study, seven layers were enough for evaluation of the stacked structure. The mean lateral periodicity of the structure (the mean lateral inter-dot distance in figure 1) was assumed to be 60 nm and it was taken into account by fixing the degrees of freedom of the nodes at the right end of the model against radial displacement. This was an additional boundary constraint to the axisymmetry of the z axis in the model. The axisymmetric eight-node bi-quadratic quadrilateral elements were employed in meshing. Young moduli of constituent materials were assumed to be 85.5 GPa for GaAs and 51.3 GPa for InAs, and Poisson ratios were 0.316 for GaAs and 0.354 for InAs. The lattice mismatch strain $\varepsilon_0 = (a_{\mathrm{GaAs}} - a_{\mathrm{InAs}})/a_{\mathrm{InAs}} = -0.067$ between the dot and matrix

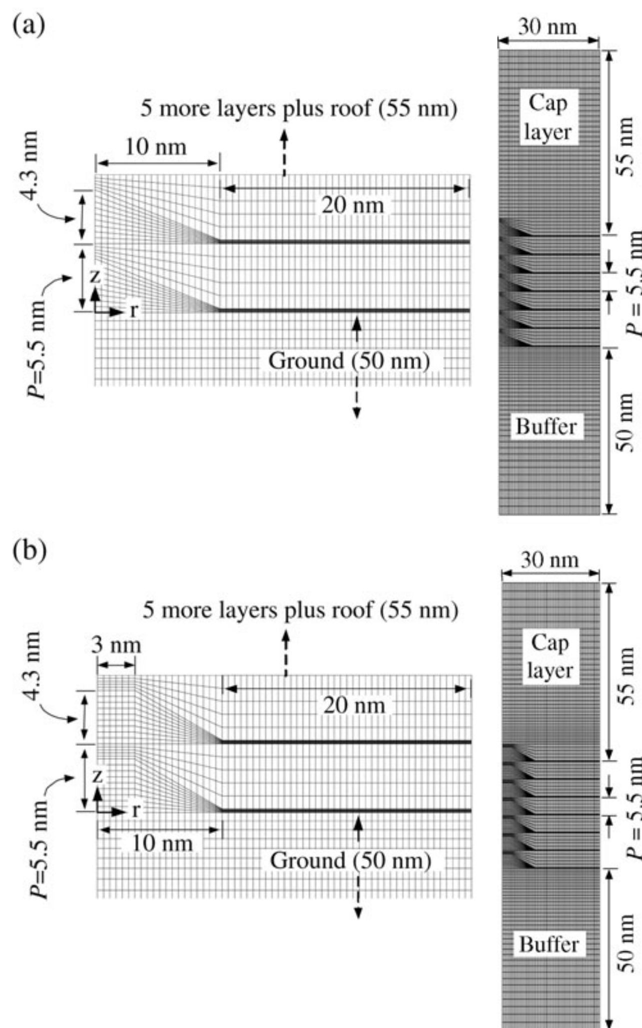

Figure 1. Geometry of models for the finite element analysis of a strain field when the vertical period of stacking is 7 nm. Stacked structures with un-truncated quantum dot (a) and with truncated quantum dot (b).

was simulated by setting the thermal expansion coefficient of the dot and the GaAs matrix to 6.7×10^{-2} and $0\ K^{-1}$, respectively, and raising the temperature by 1 K [10, 15–18]. A general-purpose commercial finite element code ABAQUS was used for calculations.

3. Results and discussion

3.1. Overall strain profiles for each shape of dot structure

It is expected that the difference in the geometry of the two types of quantum dot structures considered in this work would result in different overall strain distributions within the structures. In figure 2, the strain fields along the axial position in these two structures with the stacking period of 7 nm are compared. As can be seen, strain profiles show quite periodic characteristics

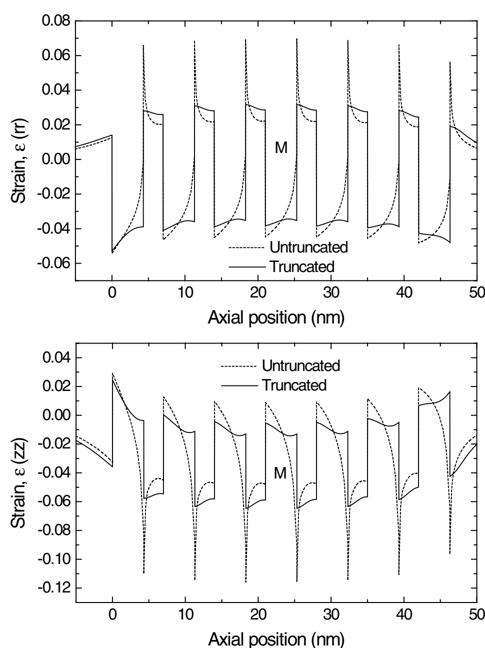

Figure 2. Strain fields along the axial position of the stacked structures with two different types of dot when the stacking period is 7 nm.

for each dot type and this was also the case for other stacking periods considered. Since the strain fields in the layers from the second to the sixth are similar both quantitatively and qualitatively, the region corresponding to the fourth (mid-) layer of the dot, denoted as 'M' in figure 2, was taken as representative of the multiple-layer-stacked structures for both the un-truncated and truncated dots. As the number of stacked layers increases, characterizing the mid-layer is more important since more layers are in a similar strain state to the mid-layer. Thus in this work, the strain fields in the fourth layers for each dot shape are further investigated for detailed analysis.

As the difference in the geometry of quantum dots resulted in different strain distributions in the structure, so did it within the dots. Figure 3 shows the strain contours in the cross section of the un-truncated and truncated quantum dots in the mid-layers for the stacking period of 7 nm. The minimum in the strain is in the apex region of the un-truncated dot whilst it is away from the centre of the truncated dot at the edge between the dot plateau and the slope. This results in a less rapid strain gradient along the axial region of the truncated dot as compared with the un-truncated one, consistent with the strain profiles in figure 2. This feature is qualitatively similar to what was shown for an unstacked single-layered dot embedded in a semi-infinite medium of a GaAs matrix in the literature [9, 10, 20]. Thus it is suggested that the overall change in strain profile with dot truncation is also maintained in the stacked structure. However, as is clear in figure 3, the magnitude of the strain at an arbitrary location in the dot is different for the two cases.

3.2. Dot strain fields at mid-layers of each dot structure

From the comparison of the strain fields in figures 2 and 3, it was predicted that radial and axial strain components ε_{rr} and ε_{zz} in two types of quantum dots are different. Hence, the difference

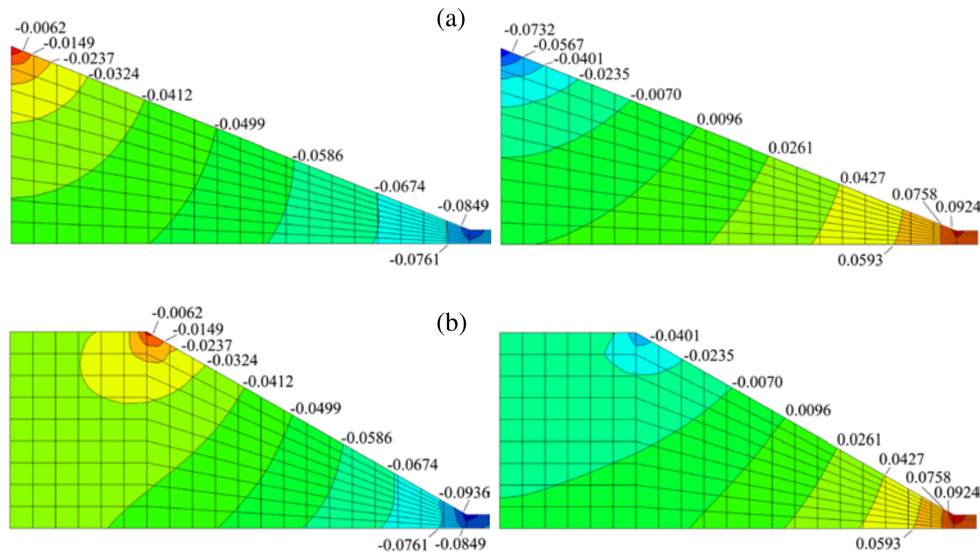

Figure 3. Contour diagrams comparing radial and axial strain components for the dots in mid-layer of the structures with an un-truncated dot (a) and truncated dot (b) when the stacking period is 7 nm.

(This figure is in colour only in the electronic version)

in ε_{hyd} and ε_{bi} between the two dot shapes is also expected as they are functions of ε_{rr} and ε_{zz} via $\varepsilon_{bi} = \varepsilon_{zz} - \varepsilon_{rr}$ and $\varepsilon_{hyd} = \varepsilon_{zz} + 2\varepsilon_{rr}$ [9]. For quantitative analysis of the strain fields, the strain components ε_{rr}, ε_{zz}, ε_{hyd} and ε_{bi} along the central axis of each dot in the mid-layers are compared in figures 4 (un-truncated) and 5 (truncated) for various stacking periods[2]. It is noted in figures 4 and 5 that the changes in strain of both types of dots in mid-layers are obvious with vertical period for ε_{rr}, ε_{zz} and ε_{bi}, while ε_{hyd} shows only a slight change. For the un-truncated dot (figure 4), the change in strain with stacking period is more apparent at the base of the dot while it shows a relatively smaller gradient across the axial position for the case of a truncated dot (figure 5). This trend is consistent both qualitatively and quantitatively with the analytical result of Pearson and Faux [20]. They reported strain profiles along the central axis of both un-truncated and truncated pyramidal dots in the mid-layer of the five-layer-stacked structure. Their results are based on a stacking period of 8 nm and are thus comparable to the similar stacking period of 7 nm in figures 4, 5.

For the quantitative characterization of the change in strain with stacking period for each type of dot in figures 4 and 5, we selected the strain value at the base of the dot in the same figures, since the strain in volume around the centre of the dot base, which takes most of the dot volume, would suitably represent the overall trend of the change in the dot strain field. Figure 6 quantifies the change in strain at this region ($r = z = 0$) as a function of stacking period P for both types of dots. As seen in the figure, the trend in strain with stacking period is qualitatively similar for the two types of dots studied herein. It is noted in figure 6(a) that the radial compressive strains, ε_{rr}, for both dots shift toward more negative values with increase in stacking period. This is because the larger volume of GaAs matrix located between

[2] In interpreting figures 4 and 5, care must be taken since the base of the dot was taken as the reference position, i.e. $z = 0$ in figures 4 and 5. This relative axial position should not be confused with the absolute origin in figure 2. Also, note that the stacking period of infinity corresponds to an unstacked single dot layer.

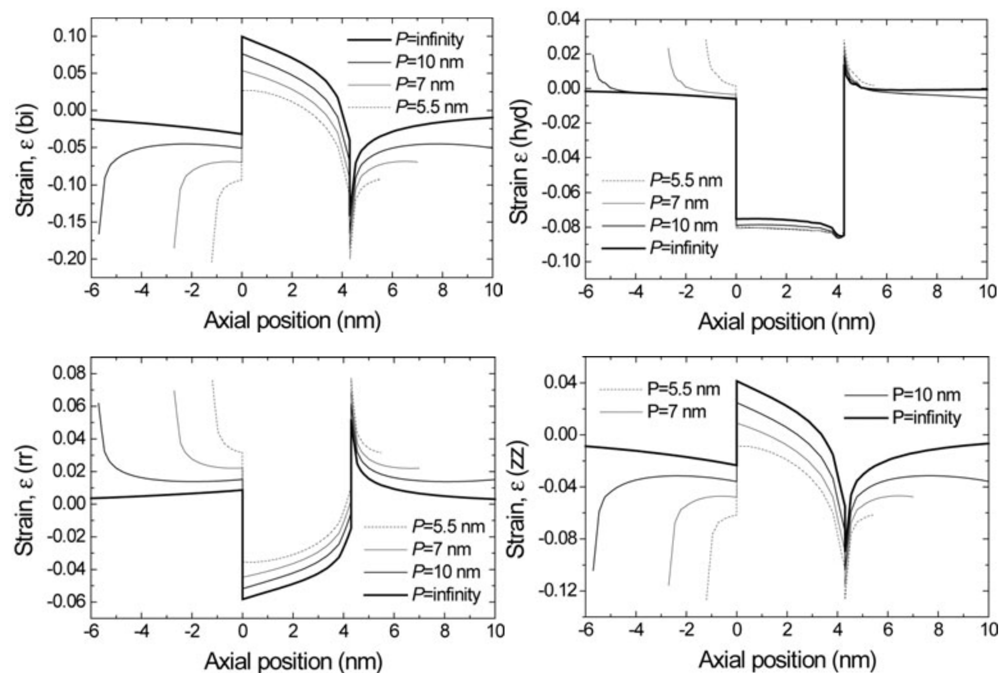

Figure 4. Comparison of the strain field in or around the mid-layer of the stacked structure with an un-truncated dot at varying stacking periods.

the vertically stacked dots prevents the expansion of the dots more efficiently when they are getting far away. The trend in vertical strains, ε_{zz}, for both dots are reversed from the radial strains due to the Poisson effect, i.e. the tensile strains ε_{zz} are becoming more tensile as the stacking period increases. However, the amount of tensile shift in ε_{zz} as P increases from 5.5 to 10 nm is about twice the amount of compressive shift in ε_{rr} for both types of dots. This would be responsible for the negligible change in hydrostatic strains ($\varepsilon_{zz} + 2\varepsilon_{rr}$) with P in figure 6(b) since the shift in ε_{zz} and $2\varepsilon_{rr}$ offset each other. For the case of biaxial strains, however, the tensile shift is most salient with P in figure 6 because the tensile shift in ε_{zz} and compressive shift in ε_{rr} reinforce the shift in ε_{bi} ($=\varepsilon_{zz} - \varepsilon_{rr}$).

The change in axial strain ε_{zz} in figure 6 can be compared with some existing work. In figure 6, ε_{zz} in a truncated dot is positive (at the dot base) for the unstacked dot (stacking period is infinity). The existing work for the unstacked and fully embedded single layered dot reports the same result [9–19]. As seen in figure 5, not only the base but also the apex is actually also positive when P is infinite. However, the tensile ε_{zz} decreases as the dots are more closely stacked (as the stacking period decreases) and then changes its sign to compressive below about 7.7 nm of stacking period (figure 6). This phenomenon is due to the interaction of the strain field originating from each stacked dot. In [20], ε_{zz} at the dot base is slightly positive (almost zero) at a stacking period of 8 nm (in mid-layer) but the minor error is acceptable for the two works based on different dot models and approaches: ours are conical dots based on FE whilst theirs are pyramidal dots based on an analytical approach. Indeed, only this much difference is found for different dot models, supporting the use of conical dot geometry and the FE approach. There has also been experimental evidence qualitatively supporting the result in figure 6, especially for ε_{zz}. In [39], the experimentally observed ε_{zz} in a multi-stacked truncated dot at a stacking period of 13 nm was also tensile, confirming the result in figure 6.

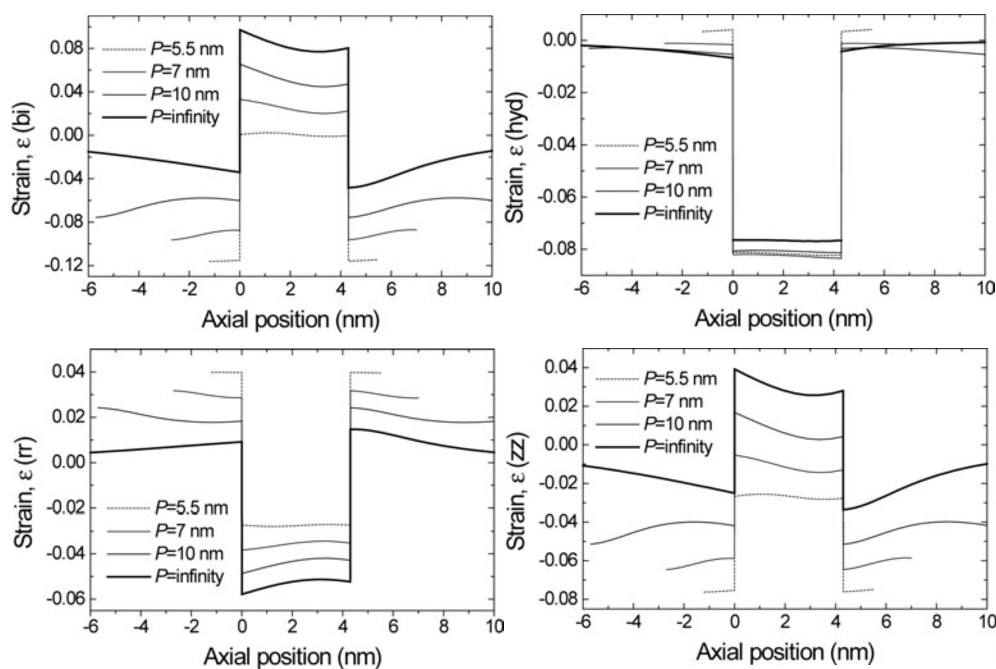

Figure 5. Comparison of the strain field in or around the mid-layer of the stacked structure with a truncated dot at varying stacking periods.

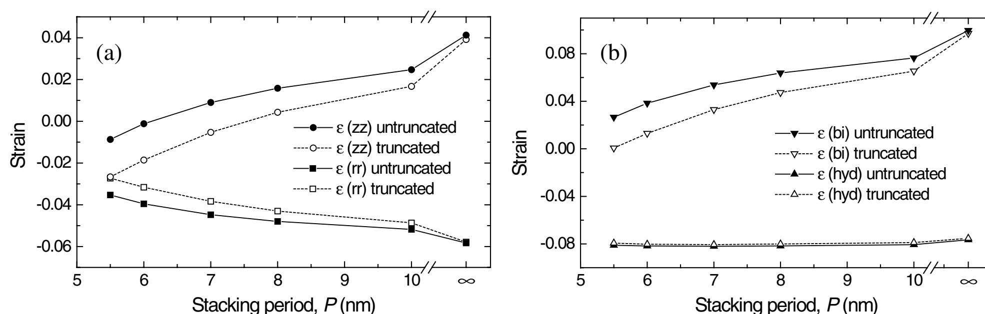

Figure 6. Comparison of four strain components at the central base of the dot ($r = 0$) for the two different types of dot at various vertical periods of stacking.

But quantitative comparison with theirs is not pursued here since their specimen was a cleaved STM sample which had different boundary conditions from the bulk specimen considered in the current work.

3.3. Comparison of strain between the two shapes of dots

So far we have discussed the change in strain at the dot base region as the stacking period increases (figure 6). Now it is necessary to discuss the difference between the dotted and full curves in figure 6, i.e. comparison between the two different dot shapes. Comparing the truncated state (dotted curve) with reference to the un-truncated state (full curve) in figure 6, it is noted that the compressive radial strain in the axial region of the truncated dot has been

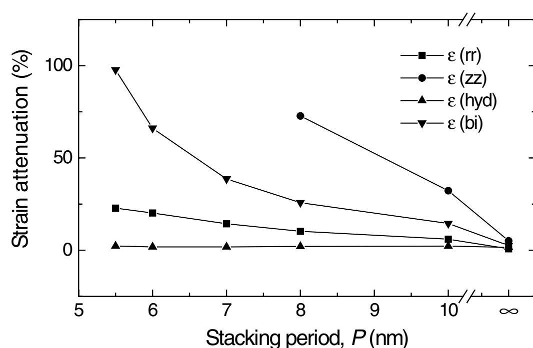

Figure 7. Change in strain attenuation due to dot truncation as a function of the stacking period.

shifted in the tensile direction (figure 6(a)), i.e. attenuated to be less compressive at various stacking periods. This is because there is less available volume of GaAs matrix to prevent the dot expansion between the vertically aligned truncated dots as compared with un-truncated ones. The change in vertical strain, ε_{zz}, with truncation is reversed from a radial strain due to the Poisson effect, i.e. the tensile ε_{zz} in figure 6(a) has shifted in the compressive direction to be attenuated as compared with the un-truncated case.

The difference between the two curves (dotted and full) in biaxial and hydrostatic strain in figure 6(b) can be explained by the very similar way that was used to explain the reason why these strains changed as the stacking period increases, as mentioned in section 3.2. The shift in hydrostatic strain from the un-truncated to the truncated state in figure 6(b) is small. This is because the amount of tensile shift (difference between the two curves) in ε_{zz} from the un-truncated state (for instance, about 0.0143 when $P = 7$ nm) is about twice the amount of compressive shift in ε_{rr} (0.0064 when $P = 7$ nm), which diminishes the change in hydrostatic strain ($\varepsilon_{zz} + 2\varepsilon_{rr}$) with truncation. For the change in biaxial strain, however, the compressive shift from the un-truncated state is most salient because the compressive shift in ε_{zz} and the tensile shift in ε_{rr} reinforce the shift in ε_{bi} ($=\varepsilon_{zz} - \varepsilon_{rr}$) with truncation as before.

It is also noted in figure 6 that the difference in ε_{rr}, ε_{zz} and ε_{bi} between the two types of the dots increases as the stacking period decreases, although that in ε_{hyd} is relatively less sensitive with the stacking period. It is thus necessary to quantify the degree of strain reduction in the truncated dot as compared with the un-truncated one at varying stacking periods. For this purpose, the reduction in strain values in a truncated dot relative to those in an un-truncated dot are shown on a percentage scale in figure 7. As seen in figure 7, the decrease in hydrostatic strain, ε_{hyd}, is trivial (about 1–2%) and roughly similar at various stacking periods whilst other strain components show significant increases in strain attenuation with decreasing P. The attenuation in axial strain ε_{zz}, biaxial strain ε_{bi} and radial strain ε_{rr} in the truncated dot is remarkable in stacked structures (as compared with unstacked states when P is infinity). For the case of biaxial strain, almost all the tensile biaxial strain is relieved when the stacking period reaches 5.5 nm and there is about 22.8% attenuation in compressive radial strain ε_{rr} at the same stacking period. As seen in figure 7, the attenuation in tensile axial strain ε_{zz} in a truncated dot is most rapid as the stacking period decreases. Actually all the tensile axial strain is relieved at 7 nm $< P <$ 8 nm (about 100%) and then the sign of strain in a truncated dot is reversed to compressive and increases in the compressive direction as the stacking period decreases further. Thus the strain attenuation when $P < 8$ nm is not shown for ε_{zz} in figure 7.

The estimation of strain attenuation so far has been based on the strain near the base ($r = z = 0$) of the dot. It is now necessary to check the trend of strain attenuation in other dot

regions by revisiting figure 3. Comparing the strain at the region common to each type of dot in figure 3, the compressive strain is indeed less compressive and the tensile one is less tensile in the truncated dot at an arbitrary dot position, confirming that the strain attenuation in the dot takes place at other dot regions as well. Looking into the truncated dot in figure 3, the strain in most of the newly present regions due to the truncation is similarly in a relaxed strain state as the neighbours except for the region of strain minimum. Such a small region, e.g. inside the contour of -0.0237 for ε_{rr} and -0.0235 for ε_{zz}, was simply shifted from the apex of the un-truncated dot and hence the overall trend of the strain attenuation in the truncated dot across the entire volume is confirmed.

3.4. Further discussions

Addressing the physical significance of such strain attenuation in a truncated dot at various stacking periods (figures 6 and 7), the significant change in strain field and associated piezoelectric potential may lead to a modification of electronic states [11] and energy level splitting [40]. Since the calculation of the optical properties for the current complicated multi-stacked structure has not been the scope of the current work, quantitative correlation of the changes in strain components to the optical properties is not pursued here. However, the negligible change in hydrostatic strain component with dot truncation (figure 7) is interpreted to yield no significant change in conduction band edges whilst the apparent attenuation in biaxial strain component with dot truncation (figure 7) is expected to alter the valence band edges significantly [12]. Since the attenuation in biaxial strain has been reported to decrease the valence band edges to increase the band gap [28, 41, 42], the case of biaxial strain herein with dot truncation is expected to yield a similar result. However, care has to be taken in predicting the actual band gap-related physical properties with truncation, such as photoluminescence properties [6, 7, 43, 44], because they are also governed by other sources such as quantum mechanical coupling between the stacked multi-dots [28] in addition to the influence of strain studied here.

3.5. Summary and conclusions

Strain fields in truncated InAs quantum dots and equivalent un-truncated ones were examined numerically. It was assumed that both of the dots have the same height (4.3 nm) and base length (20 nm) and are vertically stacked in a GaAs matrix at various stacking periods (5.5–10 nm). The comparison of the strain components was carried out for the two different types of quantum dots located in the mid-layer of the stacked structures, which is regarded as representative of the stacked nanostructures.

The compressive hydrostatic strain in a truncated dot was relieved slightly (1–2%) compared with the un-truncated one without regard to the stacking period. However, the attenuation in other strain components was significant. The attenuation for biaxial, axial and radial strains with dot truncation was minimal at the stacking period of infinity (when the structure contains an unstacked single dot layer) whilst the attenuation increased significantly as the dots were vertically stacked closer, i.e. as the stacking period decreases. The significant attenuation in strain may lead to a modification of electronic states and valence band edges to increase the band gap, whilst care has to be taken in predicting band gap-related properties with dot truncation since other sources, such as quantum mechanical tunnelling between stacked dots, can also be involved.

References

[1] Bimberg D, Grundmann M and Ledentsov N N 1998 *Quantum Dot Heterostructures* (Chichester: Wiley)
[2] Duboz J-Y, Liu H C, Wasilewski Z R, Byloss M and Dudek R 2003 *J. Appl. Phys.* **93** 1320
[3] Becker C, Sirtori C, Drachenko O, Rylkov V, Smirnov D and Leotin J 2002 *J. Appl. Phys. Lett.* **81** 2941
[4] Yang T, Kohmoto S, Nakamura H and Asakawa K 2003 *J. Appl. Phys.* **93** 1190
[5] Kim J S, Yu P W, Leem J Y, Jeon M H, Noh S G, Lee J I, Kim G H, Kang S-K, Kim J S and Kim S G 2002 *J. Appl. Phys.* **91** 5055
[6] Miller M S, Malm J-O, Pistol M E, Jeppesen S, Kowalski B, Georgsson K and Samuelson L 1996 *J. Appl. Phys.* **80** 3360
[7] Solomon G S, Trezza J A, Marshall J A and Harris J A Jr 1996 *Phys. Rev. Lett.* **76** 952
[8] Grundmann M, Stier O and Bimberg D 1995 *Phys. Rev.* B **52** 11969
[9] Stoleru V-G, Pal D and Towe E 2002 *Physica* E **15** 131
[10] Liu G R and Jerry Q 2002 *Semicond. Sci. Technol.* **17** 630
[11] Coli P and Iannaccone G 2002 *Nanotechnology* **13** 263
[12] O'Reilly E P 1989 *Semicond. Sci. Technol.* **4** 121
[13] Romanov A E, Beltz G E, Fischer W T, Petroff P M and Speck J S 2001 *J. Appl. Phys.* **89** 4523
[14] Muralidharan G 2000 *Japan. J. Appl. Phys.* **39** L658
[15] Benabbas T, Androussi Y and Lefebvre A 1999 *J. Appl. Phys.* **86** 1945
[16] Benabbas T, Francois P, Androussi Y and Lefebvre A 1996 *J. Appl. Phys.* **80** 2763
[17] Grillo V, Lazzarini L and Remmele T 2002 *Mater. Sci. Eng.* B **91/92** 264
[18] Tillmann K and Forster A 2000 *Thin Solid Films* **368** 93
[19] Downes J R, Faux D A and O'Reilly E P 1997 *J. Appl. Phys.* **81** 6700
[20] Pearson G S and Faux D A 2000 *J. Appl. Phys.* **88** 730
[21] Goldstein L, Glas F, Marzin J Y, Charasse M N and LeRoux G 1985 *Appl. Phys. Lett.* **47** 1099
[22] Xie Q, Madhukar A, Chen P and Kobayashi N P 1995 *Phys. Rev. Lett.* **75** 2542
[23] Xie Q, Chen P and Madhukar A 1994 *Appl. Phys. Lett.* **65** 2051
[24] Dvurechenskii A V, Nenashev A V and Yakimov A I 2002 *Nanotechnology* **13** 75
[25] Kikuchi Y, Suguii H and Shintani K 2001 *J. Appl. Phys.* **89** 1191
[26] Pryor C, Kim J, Wang L W, Williamson A J and Zunger A 1998 *J. Appl. Phys.* **83** 2548
[27] Faux D A, Jones G and O'Reilly E P 1994 *Modelling Simul. Mater. Sci. Eng.* **2** 9
[28] Tadic M, Peeters F M, Janssens K L, Korkusinski M and Hawrylak P 2002 *J. Appl. Phys.* **92** 5819
[29] Bernard J and Zunger A 1994 *Appl. Phys. Lett.* **65** 165
[30] Brandt O, Ploog K, Bierwolf R and Hosenstein M 1992 *Phys. Rev. Lett.* **68** 1339
[31] Eshelby J D 1957 *Proc. R. Soc.* A **241** 376
[32] Andreev A D, Downes J R, Faux D A and O'Reilly E P 1999 *J. Appl. Phys.* **86** 297
[33] Christiansen S, Albrecht M, Strunk H P and Maier H J 1994 *Appl. Phys. Lett.* **64** 3617
[34] Moreno M, Trampert A, Jenichen B, Daweritz L and Ploog K H 2002 *J. Appl. Phys.* **92** 4672
[35] Lenz A, Timm R, Eisele H, Hennig Ch, Becker S K, Sellin R L, Pohl U W, Bimberg D and Dahne M 2002 *Appl. Phys. Lett.* **81** 5150
[36] Ruvimov S and Scheerschmidt K 1995 *Phys. Status Solidi* a **150** 471
[37] Rouvimov S, Liliental-Weber Z, Swider W, Washburn J, Weber E R, Sasaki A, Wakahara A, Furkawa Y, Abe T and Noda S 1998 *J. Electron. Mater.* **27** 427
[38] Paranthoen C, Bertru N, Lambert B, Dehaese O, Le Corre A, Even J, Loualiche S, Lissillour F, Moreau G and Simon J C 2002 *Semicond. Sci. Technol.* **17** L5
[39] Legrand B, Grandidier B, Nys J P, Stievenard D, Gerard J M and Thierry-Mieg V 1998 *Appl. Phys. Lett.* **73** 96
[40] Fonseca L R C, Jimenez J L and Lebruton J P 1998 *Phys. Rev.* B **58** 9955
Fonseca L R C, Jimenez J L and Lebruton J P 1999 *Phys. Rev.* B **60** 2127
[41] Sheng W and Leburton J-P 2002 *Phys. Rev. Lett.* **88** 167401-1
[42] Korkusinski M and Hawrylak P 2001 *Phys. Rev.* B **63** 195311-1
[43] Wang B and Chua S-J 2001 *Appl. Phys. Lett.* **78** 628
[44] Xie Q, Kobayashi N P, Ramachandaran T R, Kalburge A, Chen P and Madhukar A 1996 *J. Vac. Sci. Technol.* B **143** 2203